APPLIED SCIENCES AND ENGINEERING

Foot force models of crowd dynamics on a wobbly bridge

Igor Belykh,[1]* Russell Jeter,[1] Vladimir Belykh[2,3]

Modern pedestrian and suspension bridges are designed using industry standard packages, yet disastrous resonant vibrations are observed, necessitating multimillion dollar repairs. Recent examples include pedestrian-induced vibrations during the opening of the Solférino Bridge in Paris in 1999 and the increased bouncing of the Squibb Park Bridge in Brooklyn in 2014. The most prominent example of an unstable lively bridge is the London Millennium Bridge, which started wobbling as a result of pedestrian-bridge interactions. Pedestrian phase locking due to footstep phase adjustment is suspected to be the main cause of its large lateral vibrations; however, its role in the initiation of wobbling was debated. We develop foot force models of pedestrians' response to bridge motion and detailed, yet analytically tractable, models of crowd phase locking. We use biomechanically inspired models of crowd lateral movement to investigate to what degree pedestrian synchrony must be present for a bridge to wobble significantly and what is a critical crowd size. Our results can be used as a safety guideline for designing pedestrian bridges or limiting the maximum occupancy of an existing bridge. The pedestrian models can be used as "crash test dummies" when numerically probing a specific bridge design. This is particularly important because the U.S. code for designing pedestrian bridges does not contain explicit guidelines that account for the collective pedestrian behavior.

INTRODUCTION

Collective behavior in mechanical systems was first discovered by C. Huygens some 350 years ago (*1*). He observed two pendulum clocks, suspended on a wooden beam, spontaneously synchronize. The pendula oscillated, remaining locked in antiphase, whereas the beam remained still. Pendula with the same support coupling mechanism can also oscillate in-phase, in turn making the beam vibrate in antiphase (*2*–*4*). Notably, increasing the number of in-phase synchronized pendula attached to the supporting beam leads to larger amplitudes of the swinging beam (*5*, *6*). Originating from Huygens's experiment in simple mechanical systems, the interplay between network structure and cooperative dynamics has been extensively studied (*7*–*12*), as cooperative dynamics and phase locking have been shown to play an important role in the function or dysfunction of a wide spectrum of biological and technological networks (*13*–*16*), including complex mechanical structures and pedestrian bridges (*17*).

Many bridges have experienced dramatic vibrations or even have collapsed because of the effects of mechanical resonance [see the related Wikipedia entry (*18*) for a long list of bridge failures]. There were two major causes for the dangerous vibrations: (i) pedestrian excitation of laterally unstable bridges (*19*–*21*) and (ii) wind-induced vibrations of suspension and girder bridges, including the collapse of the Tacoma Narrows Bridge (*22*–*26*).

Some of the most well-known cases of unstable pedestrian bridges are the Toda Park Bridge in Japan (*27*), the Solférino Bridge in Paris (*28*), the London Millennium Bridge (*29*), the Maple Valley Great Suspension Bridge in Japan (*30*), the Singapore Airport's Changi Mezzanine Bridge (*31*), the Clifton Suspension Bridge in Bristol, U.K. (*32*), and the Pedro e Inês Footbridge in Portugal (*33*). A recent example is the Squibb Park Bridge in Brooklyn (*34*), described in a quote from a 2014 *New York Times* report (*35*): "This barely two-year-old wooden structure, which cost $5 million, was purposefully designed to bounce lightly with the footsteps of visitors-reminiscent of trail bridges—but over time the movement has become more conspicuous." The bridge started to move too much, and not just up and down, but also side to side. The increased bouncing and swaying were a safety concern for pedestrians walking 50 feet over the park. The Brooklyn Bridge Park Corporation sought $3 million in a lawsuit against HNTB Corporation, the bridge's original designers. A new contractor, Arup, the British engineering firm that designed the London Millennium Bridge, was then hired to develop and oversee a plan to improve the stability of the Squibb Park Bridge. Arup fixed a truss-like structure beneath the bridge and added large mass dampers that reduced bouncing more than half of what it was before [see the 2017 *New York Times* report for more details (*36*)]. Three years after it initially closed for repairs, the bouncy Squibb Park Bridge reopened to the public in April 2017 (*37*).

Interest in pedestrian collective dynamics was significantly amplified by the London Millennium Bridge, which started wobbling after its opening in 2000 (*19*–*21*). Despite significant interest, the interaction between walking pedestrians and the London Millennium Bridge has still not been fully understood. The wobbling of the London Millennium Bridge is suspected to have been initiated by a cooperative lateral excitation caused by pedestrians falling into step with the bridge's oscillations (*29*, *38*–*42*). It was noted though that phase locking on the London Millennium Bridge was not perfect, and pedestrians repeatedly tuned and detuned their footstep phase with the lateral bridge motion (*43*).

This effect of lateral excitation of footbridges by synchronous walking was studied in recent papers (*29*, *38*–*42*), including modeling the crowd synchrony by phase oscillator models (*40*–*42*). These models explain how a relatively small synchronized crowd can initiate wobbling. As nice as these phase models are, they do not fully capture a bifurcation mechanism of the abrupt onset of wobbling oscillations that occurred when the number of pedestrians exceeded a critical value [about 165 pedestrians on the London Millennium Bridge (*29*)], especially in the

[1]Department of Mathematics and Statistics and Neuroscience Institute, Georgia State University, P. O. Box 4110, Atlanta, GA 30302–4110, USA. [2]Department of Mathematics, Volga State University of Water Transport, 5A Nesterov Street, Nizhny Novgorod 603951, Russia. [3]Department of Control Theory, Lobachevsky State University of Nizhny Novgorod, 23 Gagarin Avenue, Nizhny Novgorod 603950, Russia.
*Corresponding author. Email: ibelykh@gsu.edu

limiting case of identical walkers for which the phase oscillator network has no threshold for instability, and therefore the bridge would start wobbling for even a very small crowd size (*42*). Rigorous analysis of the phase model system (*40*–*42*) is based on the heterogeneity of pedestrians' frequencies, which is a natural assumption; however, the frequencies' density distribution is continuous, thereby implicitly assuming an infinite number of pedestrians. Here, we develop a biomechanically inspired model of pedestrians' response to bridge motion and detailed, yet analytically tractable, models of crowd synchrony and phase locking that take into account the timing and impact of pedestrian foot forces and assume a finite number of pedestrians. Our analysis predicts the critical number of pedestrians and its dependence on the frequencies of human walking and the natural frequency of the London Millennium Bridge remarkably well. Our results support the general view that pedestrian lock-in was necessary for the London Millennium Bridge to develop large-amplitude wobbling. However, our observations also suggest that the popular explanation that the wobbling of the London Millennium Bridge was initiated by crowd synchrony among pedestrians may be an oversimplification.

Surprisingly, the U.S. code and industry standard packages for designing pedestrian bridges do not explicitly address an impact of crowd collective behavior but rather relies on a higher nominal static pedestrian load and testing via the application of a periodic external force (*44*). The *Guide Specifications for the Design of Pedestrian Bridges* [(*44*), chapter 6] set lower limits on the fundamental frequency of a bridge in the vertical and horizontal directions to 3.0 and 1.3 Hz, respectively. However, these limits might not be respected, provided that there is "phasing of loading from multiple pedestrians on the bridge at the same time" (*44*). The code gives no specifications on how to model and describe these phase loads. In light of this, our biomechanical models of pedestrian locomotion and their bidirectional interaction with a lively bridge can be incorporated into industry standard bridge simulation packages to provide a more accurate account for the emergence of undesired crowd-induced resonant vibrations.

The layout of this paper is as follows: In the "Pendulum Models of Walker-Bridge Interactions" section, we first introduce an inverted pendulum model of pedestrian balance, where the control of the position of foot placement plays a significant role in lateral stabilization. We also propose a simplified, more analytically tractable model with a van der Pol–type oscillatory mechanism of each pedestrian's gait. In the "Predicting the Onset of Bridge Wobbling" section, we study bidirectional interactions between the van der Pol–type pedestrian models and a bridge and derive explicit analytical conditions under which phase locking and bridge wobbling appear in the system when the crowd size exceeds a threshold value. In the "Nonidentical Inverted Pendulum Walkers" section, we study the pedestrian-bridge interaction model, where pedestrians' lateral gaits are described by an inverted pendulum model. This analysis also reveals the threshold effect that induces bridge wobbling at a sufficiently large crowd size.

PENDULUM MODELS OF WALKER-BRIDGE INTERACTIONS

We model lateral oscillations of the bridge and side-to-side movement of walkers by a mass-spring-damper system (Fig. 1). The bridge is represented by a platform of mass M that moves in the horizontal direction with damping coefficient d. One side of the platform is attached to the support via a spring with elasticity k. The platform is subjected to horizontal forces, caused by the walker response to lateral bridge motion. The walkers are modeled by n self-sustained oscillators, representing walker lateral balance and capable of adjusting their footfall forces and amplitudes in response to the lateral wobbling of the bridge. The modeling equations read

$$\ddot{x}_i + f(x_i, \dot{x}_i) = -\ddot{y},\ \ \ddot{y} + 2h\dot{y} + \Omega_0^2 y = -r\sum_{i=1}^{n}\ddot{x}_i \qquad (1)$$

where the x_i equation describes the oscillatory side-to-side motion of the ith walker. The oscillatory mechanism and response of each walker's gait to the bridge's vibrations are modeled by the function $f(x_i, \dot{x}_i)$, and the effect of the bridge on the ith walker is described by the inertial feedback term $-\ddot{y}$. The y equation describes bridge oscillations. Without loss of generality, each walker is assumed to have mass m; heterogeneity of the walkers will be introduced by nonidentical gait frequencies. The ith walker applies sideways force $-m\ddot{x}_i$ to the bridge. The parameter $h = d/(2(M + nm))$ is the normalized, dimensionless damping coefficient. $\Omega_0 = \sqrt{k/(M + nm)}$ is the natural frequency of the bridge loaded with n walkers. The ratio $r = m/(M + nm)$ represents the strength of the coupling between the walkers and the bridge. Model 1 takes into account the role of walkers' footfall forces and their adaptation. It extends the models (*40*–*42*) that describe the crowd synchrony, where walkers are modeled by phase oscillators and therefore only account for the timing of each walker's gait. As in earlier studies (*40*–*42*), no person-person interactions, including visual communication between

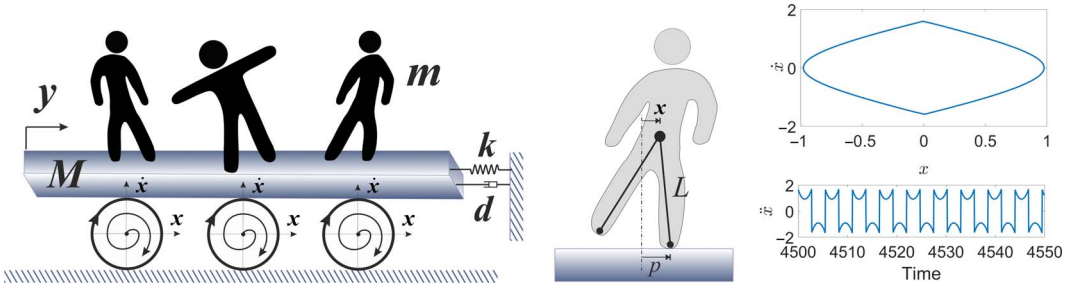

Fig. 1. A Huygens-type setup as a mechanical model for lateral vibrations of a bridge. (**Left**). The platform with mass M, a spring, and a damper represents lateral vibrations of the bridge y. Pedestrians are modeled by self-sustained oscillators, representing walker lateral balance that are capable of adjusting the position of their centers of mass and are subjected to lateral bridge motion. (**Middle**) Inverted pendulum model of pedestrian lateral movement. Variable x is the lateral position of pedestrian's center of mass. The constant p defines the lateral position of the center of pressure of the foot. L is the inverted pendulum length. (**Right**) The corresponding limit cycle in the inverted pendulum model (Eq. 3) along with its acceleration time series. Parameters are as in Fig. 8.

the walkers and moving in dense crowds at a slower pace, are included in the model (Eq. 1).

Function $f(x_i, \dot{x}_i)$, determines a self-sustained oscillatory mechanism of the ith walker gait dynamics and takes into account the role of walkers' footfall force and gait adaptation to bridge oscillations. While we anticipate that various forms of $f(x_i, \dot{x}_i)$, ensuring self-excitation of walkers' movement, can induce significant bridge oscillations via Huygens' excitation mechanism (*1*–*6*), we propose two particular types of function $f(x_i, \dot{x}_i)$ to formulate two foot force walker models. The first biomechanically inspired oscillator model is an extension of the inverted pendulum pedestrian models (*32*, *43*, *45*, *46*). The second, more analytically tractable model uses a simple van der Pol–type excitation mechanism. Represented by two different $f(x_i, \dot{x}_i)$, both models reveal similar effects and predict the critical number of walkers [$n = 165$, (*29*)], beyond which the sharp onset of wobbling occurred on the London Millennium Bridge. Our study of the inverted pendulum model also indicates that crowd phase locking stably appears in the system and supports the observation of crowd synchrony on the London Millennium Bridge, especially during large-amplitude vibrations. However, our simulations indicate that the initiation of wobbling is accompanied by multiple phase slips and nonsynchronous adjustments of pedestrian footsteps such that a phase lock-in mechanism might not necessarily be the main cause of initial small-amplitude wobbling.

Inverted pendulum walker model

Many studies in biomechanics have confirmed that an inverted pendulum model (*43*, *45*) can be successfully applied to the analysis of whole-body balance in the lateral direction of human walking (*47*–*49*). The most popular biomechanical model (*43*) of the individual walker on a rigid floor is an inverted pendulum that is composed of a lumped mass m at the center of mass supported by rigid massless legs of length L (see Fig. 1, middle). Its equations read (*43*)

$$\begin{aligned} \ddot{x} + \omega_0^2(p - x) &= 0, \text{if } x \geq 0 \text{ (right foot)} \\ \ddot{x} + \omega_0^2(-p - x) &= 0, \text{if } x < 0 \text{ (left foot)} \end{aligned} \tag{2}$$

where x and p are the horizontal displacements of the center of mass and center of pressure of the foot, respectively, and $\omega_0 = \sqrt{g/L}$, with g being the acceleration due to gravity and L being the distance from the center of mass to the center of pressure. Although this model captures the main time characteristics of human walking such as lateral displacement, velocity, and acceleration rather precisely [see the study of Bocian *et al.* (*43*) and that of Macdonald (*46*) for details], it has several limitations, especially when used in the coupled walker-bridge model (Eq. 1). From a dynamical systems theory perspective, this is a conservative system with no damping; its phase portrait is formed by three fixed points: a center at the origin, which is confined in a diamond-shape domain, bounded by the separatrices of two saddles at $(p, 0)$ and $(-p, 0)$. The periodic motion is then governed by closed conservative curves of the center fixed point. As a result, the amplitude of a walker's lateral gait depends on the initial conditions (via the corresponding level of the closed curves of the center) and is determined by the size of the first step, although this step might be too big or too small. Note $-x$, not $+x$ in Eq. 2. This implies that the solutions of each of the two systems for the right and left feet, comprising the piecewise linear system (Eq. 2), are not cosine and sine functions as with the harmonic oscillator but instead hyperbolic functions. Therefore, the closed curves, "glued" from the solutions of the two systems, have a distinct diamond-like shape, yielding realistic time series for lateral velocity and acceleration of human walking (see Fig. 1, right).

We propose the following modification of the pedestrian model (Eq. 2) to make it a self-sustained oscillator

$$\begin{aligned} \ddot{x} &= \omega_0^2(x - p) - \lambda(\dot{x}^2 - \nu^2(x - p)^2 + \nu^2 a^2)\dot{x}, \text{if } x \geq 0 \text{(right foot)} \\ \ddot{x} &= \omega_0^2(x + p) - \lambda(\dot{x}^2 - \nu^2(x + p)^2 + \nu^2 a^2)\dot{x}, \text{if } x < 0 \text{(left foot)} \end{aligned} \tag{3}$$

where λ is a damping parameter, and parameter ν controls the period of the limit cycle. The auxiliary parameter a controls the amplitude of the limit cycle (lateral foot displacement) via the difference $(p - a)$ [see the study of Belykh *et al.* (*50*) for details].

Note that System 3 has a stable limit cycle (Fig. 1, right), which coincides with a level of the nonlinear center of the conservative System 2 for $\nu = \omega_0$. The period of the limit cycle can be calculated explicitly as the limit cycle is composed of two glued solutions for the right and left foot systems where $x = a \cosh \nu t$ and $\dot{x} = a\nu \sinh \nu t$ (for $\nu = \omega_0$) correspond to one side of the combined limit cycle, glued at $x = 0$. The use of System 3 instead of the conservative System 2 in the coupled system allows one to analyze the collective behavior of the walker-bridge interaction much more effectively, yet preserves the main realistic features of human walking. System 3 can also be written in a more convenient form

$$\ddot{x} + \lambda(\dot{x}^2 - \nu^2 x^2 + \nu^2 a^2)\dot{x} - \omega_0^2 x = 0, \quad x + p (\mathrm{mod}\, 2p) \tag{4}$$

defined on a cylinder and obtained by shifting x to $x + p$. As a result, the two saddles shift to $x = 0$ and $x = 2p$, and the limit cycle becomes centered around $x = p$. In the following, we will use Eq. 3 as the main model of the individual walker in our numerical studies of the coupled walker-bridge model (Eq. 1) with $f(x_i, \dot{x}_i)$, defined via the right-hand side (RHS) of Model 3. The analytical study of the coupled model (Eqs. 1 to 4) is somewhat cumbersome and will be reported in a more technical publication; we will further simplify the walker-bridge model (Eqs. 1 to 4), incorporating a van der Pol–type excitation mechanism and making the analysis more elegant and manageable.

Van der Pol–type walker model

An oscillatory mechanism of each walker's gait, modeled by the function $f(x_i, \dot{x}_i) = \lambda(\dot{x}_i^2 - \nu^2 x_i^2 + \nu^2 a^2)\dot{x}_i - \omega_0^2 x_i$ in Eq. 4, can be similarly described by the van der Pol–type term $f(x_i, \dot{x}_i) = \lambda_i(\dot{x}_i^2 + x_i^2 a^2)\dot{x}_i + \omega_i^2 x_i$. Therefore, the walker-bridge model (Eqs. 1 to 4) can be transformed into the following system

$$\begin{aligned} \ddot{x}_i + \lambda_i(\dot{x}_i^2 + x_i^2 - a^2)\dot{x}_i + \omega_i^2 x_i &= -\ddot{y} \\ \ddot{y} + 2h\dot{y} + \Omega^2 y &= -r\sum_{i=1}^{n} \ddot{x}_i \end{aligned} \tag{5}$$

where the dimensionless time $\tau = \nu t$, $\omega_i = \omega_0^{(i)}/\nu$, and $\Omega = \Omega_0/\nu$. Walkers are assumed to have different parameters ω_i, randomly distributed within the range $[\omega_-, \omega_+]$. In relation to the frequency of pedestrian walking, parameter ω_i does not directly set the actual footfall frequency of the ith pedestrian because this frequency is also controlled by parameters a and λ. In the absence of bridge movement, the ith van der Pol–type oscillator has a limit cycle with a frequency that lies within or near the interval $(\omega_i, 1)$ (see Materials and Methods

for the justification). Note that the equations for the limit cycle of the individual van der Pol–type oscillator cannot be found explicitly, yet we will be able to find phase-locked solutions in the coupled pedestrian-bridge model (Eq. 5).

It is important to emphasize that this model is an extension of the London Millennium Bridge reduced (phase) models (*40*–*42*), where the dynamics of each walker is modeled by a simple phase oscillator with phase Θ_i. In terms of Model 5, the Eckhardt *et al.* model (*41*, *42*) reads $\dot{\Theta}_i = \omega_i - c_i\ddot{y}\cos\Theta_i; \ddot{y} + 2h\dot{y} + \Omega_0^2 y = c\sum_{i=1}^{n}\cos\Theta_i$, where ω_i is the natural stepping frequency of walker i, c_i is a coupling constant reflecting the strength of the response of walker i to a lateral force, and c is the maximum sideways force of walker i applied to the bridge. The frequencies ω_i are randomly chosen from a continuous density distribution $P(\omega)$, thereby assuming an infinite number of pedestrians. The Eckhardt *et al.* model allows for a reduction to a Kuramoto-type network and derivation of analytical estimates on the degree of coherence among the phase oscillators that causes the bridge oscillations to amplify. That is, the wobbling begins as a Kuramoto-type order parameter gradually increases in time when the size of the synchronized group increases in time (*40*–*42*). However, these phase models, based on the widespread notion of footstep phase adjustment as the main mechanism of synchronous lateral excitation, have the abovementioned limitations, including the absence of a threshold on the critical number of identical pedestrians, initiating abrupt wobbling. The presence of the feedback term $\ddot{y}$ in the x_i- equation of Model 5 has been the main obstacle, preventing the rigorous transformation of Eq. 5 to an analytically tractable model in polar coordinates. Because these limitations call for more detailed models, also taking into account foot forces and position of foot placement, we use the biomechanically inspired model (Eqs. 1 to 4) and its van der Pol–type simplification (Eqs. 1 to 5) to make progress toward a mathematical understanding of the mechanism of the London Millennium Bridge's vibrations. We begin with rigorous analysis of the model (Eqs. 1 to 5) and its implications to the London Millennium Bridge. We will derive an explicit bound on the critical crowd size needed for the onset of wobbling in the case of both identical and nonidentical pedestrians. We will also numerically validate this bound for both the inverted pendulum and the van der Pol–type models and obtain an excellent fit.

PREDICTING THE ONSET OF BRIDGE WOBBLING

It is important to emphasize that this high-dimensional, nonlinear pedestrian-bridge model (Eq. 5) is not expected to be analytically tractable in general. As a result, finding a closed-form analytical solution that corresponds to phase-locked behavior at an unknown common frequency seems to be out of reach for the existing methods. Pedestrian-bridge interactions in Model 5 are strong and the model contains no small parameters. Therefore, the averaging methods that are typically used in the Kuramoto-type phase models (*40*–*42*) or phase models of Josephson junctions with a common load (*51*) to identify the common frequency of phase locking cannot be applied. Instead, we will solve the inverse problem and synthesize an analytical solution that generates phase locking at a desired, predefined frequency. Toward this goal, we will derive explicit conditions on the intrinsic parameters of pedestrians, the bridge, and the crowd size under which this phase-locked solution appears in the system (Eq. 5) when the crowd size exceeds a threshold value. This periodic solution is induced by the adjustment of pedestrians' frequencies to the frequency of the bridge, yielding the one-to-one phase locking frequency ratio between the pedestrians and the bridge.

We seek the periodic solutions in the form

$$x_i(t) = B_i\sin(t+\varphi_i) \text{ and } y(t) = A\sin(t+\psi) \tag{6}$$

where B_i and φ_i are the amplitude and phase of the ith oscillator (pedestrian) and A and ψ are related to the bridge. We have set the frequency of the pedestrian-bridge phase-locked motion equal to 1. The harmonic solutions x_i and y with frequency equal to 1 do not exist in the pedestrian-bridge model (Eq. 5) with arbitrarily chosen frequencies of the pedestrians and the bridge. However, we will give an explicit recipe of how to choose the intrinsic parameters that yield and preserve the harmonic solutions x_i and y with frequency equal to 1 when the crowd size increases. Therefore, we will be able to conduct the assumed harmonic solutions through the "eye of the needle" of the otherwise analytically intractable model (Eq. 5) and demonstrate that these phase-locked solutions appear when the number of pedestrians exceeds the threshold value, causing an abrupt onset of bridge wobbling.

Identical van der Pol–type walkers

Analytical predictions

We begin with the worst-case scenario for the onset of wobbling, caused by identical pedestrians with uniform $\omega_i = \omega$, when, for example, British Royal Guards nearly equal in size and weight walk across the bridge, breaking step. This case is out of reach for the phase oscillator models that would become phase-locked at an infinitesimal crowd size (*40*–*42*), similar to the Kuramoto model with uniform ω that synchronizes at infinitesimally small coupling values (*52*).

The phase-locked solutions (Eq. 6) in the pedestrian-bridge model (Eq. 5) with identical oscillators correspond to complete synchronization among the pedestrians such that $x_1 = \ldots = x_n = x(t) = B\sin(t+\varphi)$ and $y(t) = A\sin(t+\psi)$ as $B_i = B$ and $\varphi_i = \varphi$, $i = 1,\ldots, n$. Substituting the solutions for x and y along with their derivatives into the first equation of System 5 yields

$$B(\omega^2-1)\sin(t+\varphi) + \lambda B(B^2-a^2)\cos(t+\varphi) = A\sin(t+\psi) \tag{7}$$

Introducing the angle β such that

$$\cos\beta = \frac{\omega^2-1}{\sqrt{(\omega^2-1)^2+\lambda^2(B^2-a^2)^2}}, \quad \sin\beta = \frac{\lambda(B^2-a^2)}{\sqrt{(\omega^2-1)^2+\lambda^2(B^2-a^2)^2}} \tag{8}$$

we obtain

$$B\sqrt{(\omega^2-1)^2+\lambda^2(B^2-a^2)^2}[\cos\beta\sin(t+\varphi)+\sin\beta\cos(t+\varphi)] = A\sin(t+\psi) \tag{9}$$

Using a trigonometric identity $\cos\beta\sin(t+\varphi)+\sin\beta\cos(t+\varphi) = \sin(t+\varphi+\beta)$, we turn Eq. 9 into

$$B\sqrt{(\omega^2-1)^2+\lambda^2(B^2-a^2)^2}\sin(t+\varphi+\beta) = A\sin(t+\psi)$$

This equation holds true if

$$A = B\sqrt{(\omega^2-1)^2+\lambda^2(B^2-a^2)^2}, \text{and } \beta = \psi - \varphi$$

Taking into account Eq. 8, we obtain the following equations for amplitude and phase balances between the pedestrians and the bridge

$$A = \sqrt{B^2(\omega^2-1)^2+\lambda^2(B^2-a^2)^2B^2} \tag{10}$$

$$\tan(\varphi-\psi) = -\lambda\frac{B^2-a^2}{\omega^2-1} \tag{11}$$

Clearly, we need extra balance equations to identify the unknown parameters A, B, φ, and ψ. Similarly, substituting the solutions into the second equation of Eq. 5, we obtain

$$A = \frac{rn}{\sqrt{\Delta}}B \tag{12}$$

$$\tan(\varphi-\psi) = \frac{2h}{1-\Omega^2} \tag{13}$$

where $\Delta = (\Omega^2-1)^2 + 4h^2$.

Comparing the amplitude balance equations (Eqs. 10 and 12) yields

$$B^2 = a^2 + \frac{1}{\lambda}\sqrt{\frac{(rn)^2}{\Delta}-(\omega^2-1)^2} \tag{14}$$

Therefore, a necessary condition for the existence of the phase-locked solutions $x(t)$ and $y(t)$, allowing the x amplitude to be a real value, is $\frac{(rn)^2}{\Delta} \geq (\omega^2-1)^2$. This condition gives the following bound on the pedestrians $n > n_c$, required for the phase-locked solution to exist, where exceeding the critical crowd size n_c leads to the abrupt onset of bridge wobbling

$$\frac{mn_c}{mn_c+M} = |\omega^2-1|\sqrt{(\Omega^2-1)^2+4h^2} \tag{15}$$

Note that setting $\omega = 1$ yields the critical crowd size $n_c = 0$. Recall that in the absence of bridge movement, the footfall frequency of the pedestrian is equal to 1 when $\omega = 1$. As a result, Eq. 15 suggests the absence of a critical crowd size only when the pedestrian frequency ($\omega = 1$) is perfectly tuned to the bridge. In the following subsection, we will support this claim by numerically confirming the presence of a nonzero, critical crowd size in the case of identical pedestrians with $\omega \neq 1$.

Figure 2 illustrates this condition and presents mutual arrangements of the amplitude balance curves (Eqs. 10 and 12) as a function of the crowd size n. Intersections between the cubic-like curve $A = \sqrt{B^2(\omega^2-1)^2+\lambda^2(B^2-a^2)^2B^2}$ (blue line) and a straight line $A = \frac{rn}{\sqrt{\Delta}}B$ (dashed black) correspond to the existence of the phase-locked solutions (Eq. 6). The parameters are chosen to make n_c = 165 (*29*), beyond which the sharp onset of wobbling occurred on the London Millennium Bridge. For $n < 165$, the slope of the straight line is not large enough to ensure the intersection with the cubic-like curve, whereas $n_c = 165$ yields the emergence of the phase-locked solution (Eq. 6) and initiates bridge wobbling.

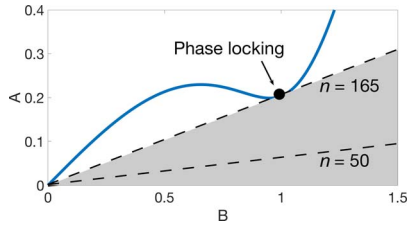

Fig. 2. Illustration of the amplitude balance conditions (Eqs. 10 and 12). The light gray area indicates the absence of wobbling, guaranteed by Eq. 15. Intersections between the blue (solid) curve (Eq. 10) and a dashed line (Eq. 12) generate phase-locked solutions for the number of pedestrians exceeding a critical number n_c = 165. Parameters are as in Fig. 3.

However, for the phase-locked solution (Eq. 6) with frequency equal to 1 to exist for $n \geq n_c$, an additional constraint such as the phase balance must be imposed. Comparing the phase balance equations (Eqs. 11 and 13), we obtain

$$B^2 = a^2 + \frac{2h(\omega^2-1)}{\lambda(\Omega^2-1)} \tag{16}$$

Equating the RHSs of Eqs. 14 and 16, we derive the following expression that links the parameters of the pedestrians and the bridge and indicates, in particular, how parameter ω should be chosen to satisfy the amplitude-phase balances (Eqs. 13 to 16)

$$\omega^2 = 1 + \frac{mn}{C(mn+M)}, \text{where } C = \Omega^2 - 1 + \frac{4h^2}{\Omega^2-1} \tag{17}$$

Numerical verification: Phase locking at frequency equal to 1

To test our analytical prediction (Eqs. 15 to 17), we have performed a series of numerical simulations (see Fig. 3) that reveal a sharp onset of bridge wobbling when the crowd size exceeds its critical value $n_c = 165$. This onset is induced by the emergence of phase locking among the pedestrians and the bridge at the predefined frequency equal to 1. For this solution to exist for $n \geq n_c = 165$, we calculate the value of ω via the amplitude-balance condition (Eq. 17). For the range of crowd sizes $n \in [1,165]$ that involves the abrupt transition from the absence of wobbling to significant wobbling, we choose and fix $\omega = 1.097$ via Eq. 17 using $n = 165$ and the parameters given in Fig. 3. This guarantees that the desired phase-locked solution with frequency equal to 1 does not exist for $n < 165$ and emerges at $n = 165$. To preserve the existence of phase-locked solution for large crowd sizes $n > 165$, we vary ω via Eq. 17 for each $n > 165$ to satisfy the balance condition (Eq. 17). This increases ω from 1.098 to 1.15 when n increases from 166 to 300. Note that the analytical conditions (Eqs. 15 to 17) only guarantee the existence or absence of the phase-locked solution for a given n and do not account for its stability. The pedestrian-bridge model (Eq. 5) contains a free parameter λ that is not explicitly present in the existence conditions (Eqs. 15 to 17), so it can be tuned to make the desired phase-locked

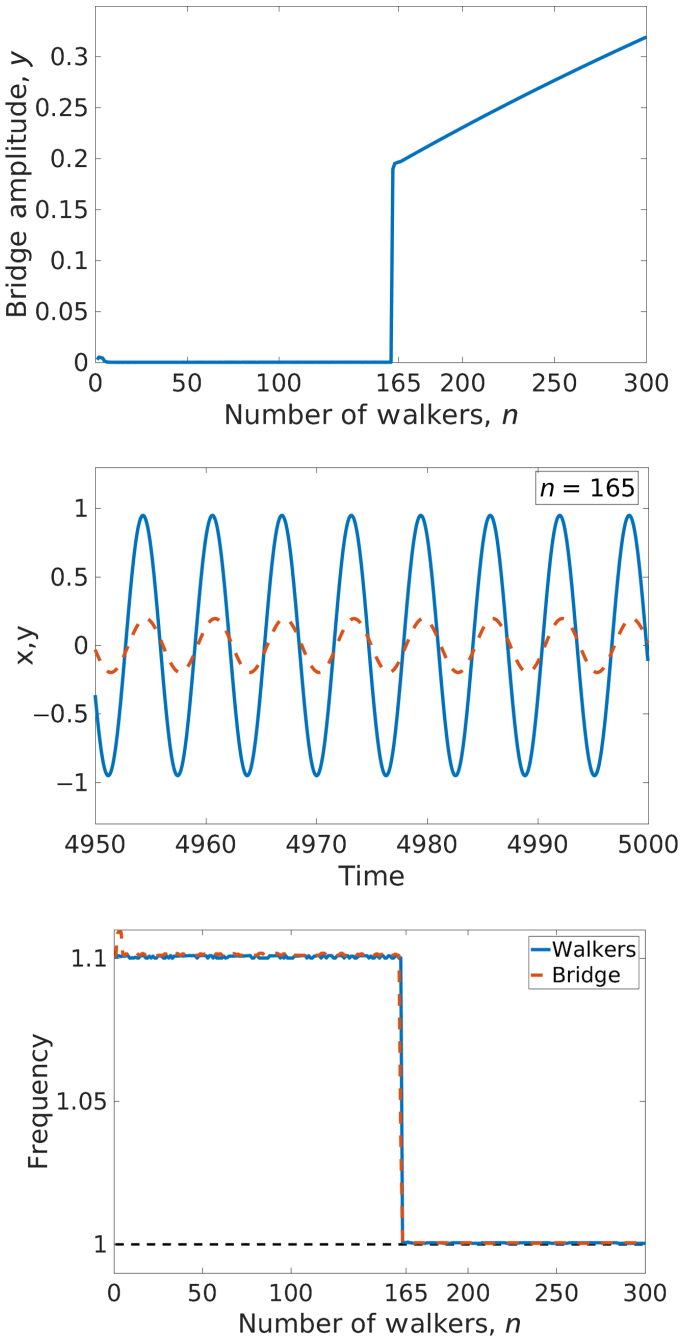

Fig. 3. Numerical verification of the analytical prediction (Eqs. 15 to 17): Phase locking with frequency equal to 1. (**Top**) Abrupt onset of bridge wobbling from random initial conditions as a function of the number of walkers in the van der Pol–type pedestrian-bridge model (Eq. 5). (**Middle**) Time series of phase locking among the pedestrians (blue solid line) and with the bridge (red dashed line) at the common frequency equal to 1 and $n = 165$. (**Bottom**) Adjustment of the averaged pedestrian and bridge frequencies. Note the bridge frequency jitters due to bridge beating before the onset of phase locking. The emergence of phase locking at frequency equal to 1 at $n = 165$ is in perfect agreement with the analytical prediction. Parameters are $\Omega = 1.2$, $\lambda = 0.5$, $h = 0.05$, $m = 70$, $M = 113{,}000$, and $a = 1.0$. For $n \in [1{,}165]$, parameter $\omega = 1.097$ is fixed and chosen via Eq. 17 to ensure that the phase-locked solution appears at $n_c = 165$. For $n \in [166{,}300]$, ω is varied via Eq. 17 to preserve the amplitude-phase balance.

solution to become stable. The phase solution with frequency equal to 1 becomes stable in a wide range of parameter λ, for example, for $\lambda \in [0.1{,}0.7]$. Therefore, we made little effort to tune λ to 0.5. Our multiple repetitive simulations from random initial conditions with $x_i(0)$, $i = 1,\ldots,$ n chosen from the range $[-1,1]$ have indicated the emergence of the same stable phase-locked rhythm, suggesting that the phase-locked solution is globally stable.

Phase locking at a different frequency

The above analysis provides a clear example of the threshold effect when the increasing crowd size induces the abrupt onset of bridge wobbling. This onset is caused by the emergence of phase locking among the pedestrians and the bridge. According to our analysis and numerics, this phase locking occurs at frequency equal to 1 if the intrinsic parameters of the pedestrian motion and the bridge are chosen in accordance with the balance condition (Eq. 17).

A natural question that arises in this context is whether the pedestrian-bridge system (Eq. 5) still exhibits the threshold effect and the emergence of phase locking if the balance condition cannot be met. In the following, we will give a positive answer to this question and demonstrate that although our analytical conditions are no longer applicable, the pedestrian-bridge system can still be tuned to exhibit the very same effect of phase locking. However, this phase locking occurs at a different frequency that can only be assessed numerically. This does not come as a surprise, given the complexity of the nonlinear system (Eq. 5) with arbitrarily chosen parameters. Nevertheless, approximate balance conditions similar to Eqs. 10 and 12 could be derived for phase-locked solutions with frequencies close to 1 by using perturbation analysis and Fourier series expansion.

In our numerical simulations, we knowingly consider the worst-case scenario and set the natural bridge frequency $\Omega = 1$ at which the balance condition (Eq. 17) has a singularity and is undefined. As a result, the analytical conditions (Eqs. 15 to 17) cannot be satisfied. Yet, the pedestrian-bridge system (Eq. 5) can be tuned to exhibit phase-locked oscillations and therefore induce bridge wobbling at the desired critical number of pedestrians $n_c = 165$, but at a frequency different from 1. Similarly to Fig. 3, Fig. 4 (top) indicates the abrupt onset of wobbling after the number of walkers exceeds the threshold ($n_c = 165$; blue, solid curve). Notice the presence of a hysteretic transition, where threshold values at which wobbling occurs and disappears depend on the direction of change of the crowd size. That is, decreasing the number of pedestrians below the threshold value $n_c = 165$ induces a hysteric transition between nonwobbling and wobbling states where the wobbling persists (black, dashed curve) until the crowd size drops below $n = 135$. Figure 4 (middle) displays the evolution of the average phase difference $\Delta\Phi = \frac{\sum_{i \neq j} |\varphi_i - \varphi_j|}{n(n-1)}$, where φ_i is the normalized phase for walker x_i. The onset of bridge wobbling coincides with complete phase locking among the pedestrians ($\Delta\Phi = 0$) at $n_c = 165$; however, decreasing n down to $n = 135$ preserves significant wobbling, accompanied by phase locking with $\Delta\Phi \neq 0$. To support this claim, Fig. 4 (bottom) shows that the largest transversal Lyapunov exponent $\lambda_\perp$ for the stability of complete phase locking among the pedestrians is negative only for $n \geq 165$. The numerical simulations of the hysteretic transition of Fig. 4 (top and middle) were performed by (i) using random initial conditions $x_i(0) \in [-1,1]$ in the direction of increasing n and (ii) perturbing the solution by adding randomly chosen $\Delta x_i(0) \in [-0.1, 0.1]$ to disrupt potential initial phase locking when decreasing n.

In addition to the threshold effect of adding and removing pedestrians from the bridge, Fig. 4 (top) shows a minor increase in bridge

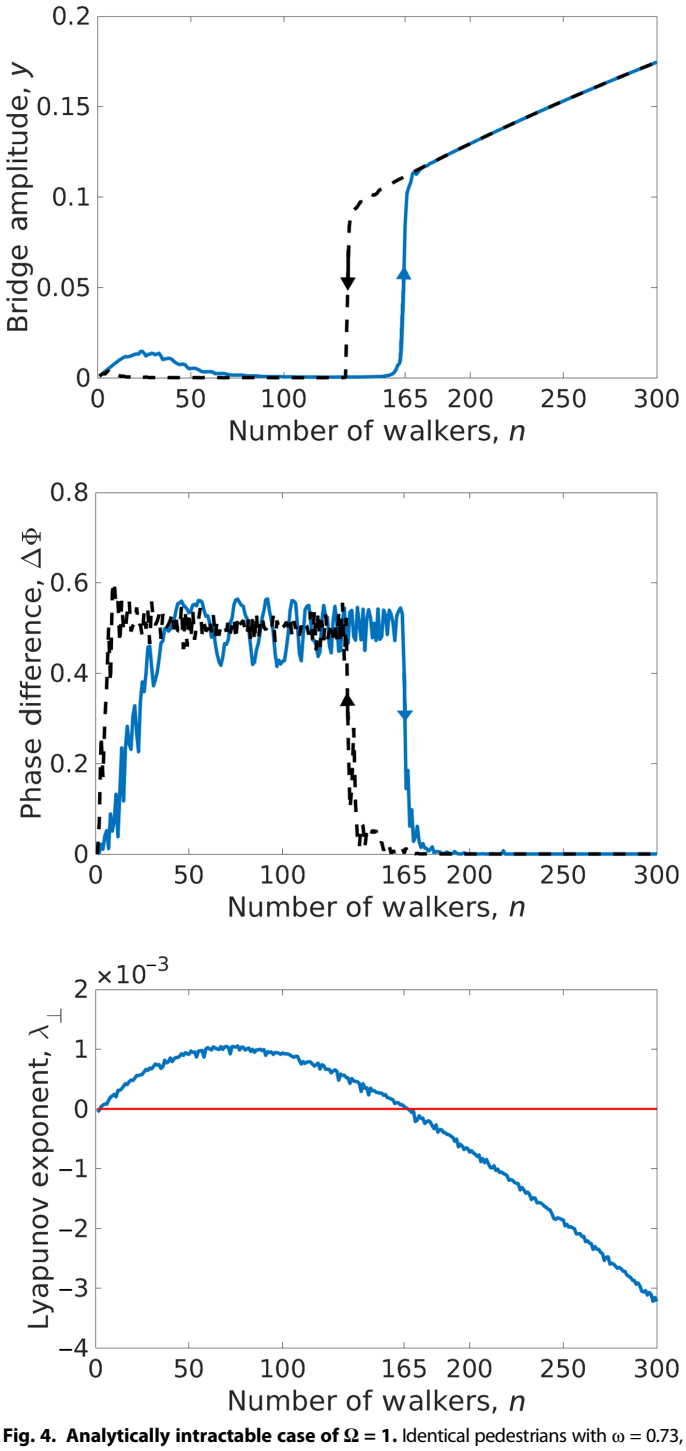

Fig. 4. Analytically intractable case of Ω = 1. Identical pedestrians with ω = 0.73, λ = 0.23, and a = 1. Other parameters are chosen to fit the data for the London Millennium Bridge: h = 0.05, M = 113,000, and m = 70. (**Top**) A hysteretic transition between nonwobbling and wobbling states as a function of crowd size n. Increasing (decreasing) n leads to the onset (termination) of bridge wobbling at n = 165 (n = 135). Notice the appearance and disappearance of the small bump in bridge wobbling $n \in$ [10,40] due to a chimera state where a subgroup of pedestrians becomes phase-locked. (**Middle**) Corresponding average phase difference ΔΦ among pedestrians' movement. (**Bottom**) The largest transversal Lyapunov exponent $\lambda_\perp$ for the stability of complete phase locking between pedestrians. Its negative values (occurring around $n \approx 165$) indicate the stability of the phase-locked solution.

wobbling oscillations for $n \in$ [10,40]. This increase is caused by a cluster of phase-locked walkers paired with a cluster of unsynchronized walkers. In dynamical systems literature, this pairing of a synchronized cluster with an asynchronous cluster (despite the homogeneity of oscillators) is often called a "chimera" state (*53*) and was also observed in experimental setups involving mechanical oscillators coupled through swings (*54*, *55*). Notice that this cluster of phase-locked pedestrians disintegrates with a further increased crowd size and stops this low-amplitude wobbling, until the critical crowd size n_c = 165 is reached.

To give more details on the onset of pedestrian phase locking, Fig. 5 shows the transition from the asynchronous pedestrian motion to fully phase-locked pedestrian behavior for crowd sizes right below and above the threshold value n_c when the crowd size increases. Because the balance conditions (Eqs. 10 and 12) for the chosen set of parameters with Ω = 1 cannot be met, phase locking occurs at a frequency different from 1 (Fig. 6). Figure 6 also shows that after the onset of phase locking, the addition of more pedestrians causes the period of oscillations for both the pedestrians and the bridge to increase as the pedestrian-bridge system becomes heavier. This generates the increase in the amplitude of bridge oscillations shown in Fig. 4.

Nonidentical van der Pol–type walkers

Our theory can also be extended to the pedestrian-bridge system (Eq. 5) with nonidentical pedestrians who have different ω_i, randomly distributed within the range $[\omega_-,\omega_+]$. Following the steps of the above study, we seek to determine the conditions that yield phase-locked solutions $x_i(t) = B_i \sin(t+\varphi_i)$, $i = 1,\ldots,n$ and $y(t) = A \sin(t+\psi)$ and reveal the threshold effect, which induces bridge wobbling at a sufficiently large crowd size.

Substituting these solutions for x_i and y into System 5, we obtain the balance conditions, similar to those from the identical pedestrian case

$$A^2 = B_i^2(\omega_i^2 - 1)^2 + \lambda^2(B_i^2 - a^2)^2 B_i^2 \tag{18}$$

$$\tan(\varphi_i - \psi) = -\lambda \frac{B_i^2 - a^2}{\omega_i^2 - 1} \tag{19}$$

$$A^2 = \frac{(rn)^2}{\Delta}\bar{B}^2 \tag{20}$$

$$\tan(\bar{\varphi} - \psi) = \frac{2h}{1 - \Omega^2} \tag{21}$$

where $\bar{B} = \frac{1}{n}\sum_{i=1}^{n} B_i$ and $\bar{\varphi} = \frac{1}{n}\sum_{i=1}^{n} \varphi_i$ are the mean amplitude and phase of the group of pedestrians, respectively. Our goal is to identify the amplitudes B_i and φ_i that are consistent with the amplitude and phase conditions (Eqs. 18 and 19) and at the same time yield the desired $\bar{B}$ and $\bar{\varphi}$ to satisfy Conditions 20 and 21. Toward this goal, we compare the amplitude conditions (Eqs. 18 to 20)

$$B_i^2(\omega_i^2 - 1)^2 + \lambda^2(B_i^2 - a^2)^2 B_i^2 = \frac{(rn)^2}{\Delta}\bar{B}^2 \tag{22}$$

Solving this equation graphically (Fig. 7), we obtain a cubic strip of the balance curves ω_i that represent the left-hand side (LHS) of

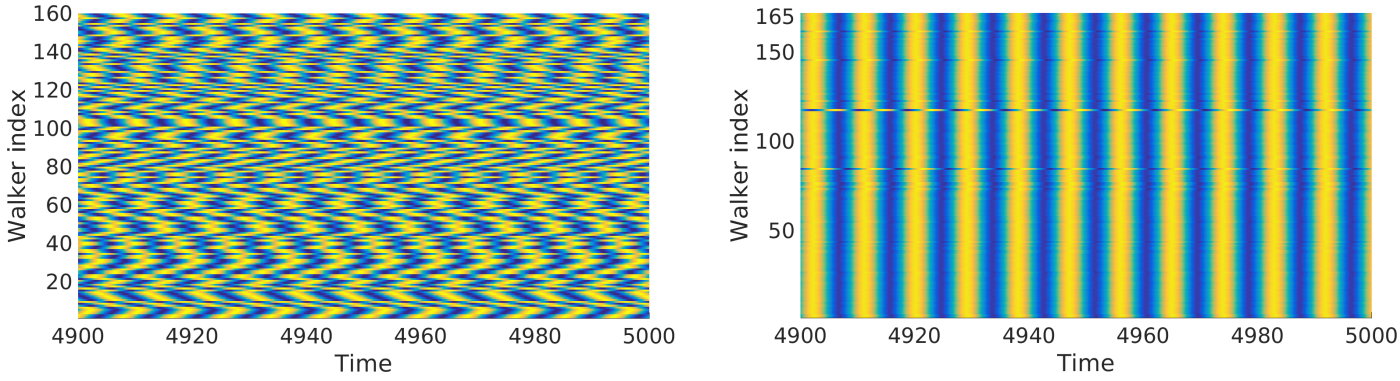

Fig. 5. Pedestrian motions represented by an amplitude color plot for a crowd size before (n = 160) (left) and after n = 166 (right) the onset of phase locking at the critical number of walkers ($n \approx 165$). The full video demonstrating the onset of phase locking as a function of the addition of pedestrians on the bridge for identical models (Eq. 5) is given in the Supplementary Materials.

Eq. 22 and a horizontal balance line defined by the RHS of Eq. 22. The intersection point between the balance curve ω_i and the horizontal line yields the amplitude B_i for the phase-locked oscillation $x_i(t)$. Similarly to the identical pedestrian case, Fig. 7 reveals the bifurcation mechanism for the abrupt onset of the bridge wobbling, defined by phase locking among all n oscillators that appears when n exceeds the critical number n_c [when the horizontal balance line (Eq. 20) intersects the upper curve ω_+]. Note that the intersections with the left and middle branches of the cubic line ω_+ also yield permissible solutions; however, they are unstable and a saddle, respectively. When the horizontal balance line (Eq. 12) intersects the cubic stripe at a level between n^* and n_c, only a fraction of balance curves with ω_i lie above this line such that only a group of pedestrians is phase-locked and only small-amplitude wobbling can appear from this partially phase-locked state.

A potential problem in solving Condition 22 for B_i^2 is that the mean amplitude $\bar{B}$ is a function of B_i, i = 1,.., n. Therefore, the values B_1, B_2,..., B_n, which are obtained from the intersections of the corresponding curves, do not necessarily sum up to match $\bar{B}$. To go around this problem, we do the following. Given the values B_1, B_2,..., B_n, we calculate its exact mean amplitude $\bar{B}$. This value differs from the original value of $\bar{B}$ that was initially chosen to set the level of the horizontal line $A^2 = \frac{(rn)^2}{\Delta}\bar{B}^2$, which generated B_1, B_2,..., B_n. To resolve this issue, we can always adjust the parameter Δ, by varying Ω or h to preserve the same level of the horizontal line $A^2 = \frac{(rn)^2}{\Delta}\bar{B}^2$, with the updated mean amplitude $\bar{B}$, which matches the values of B_1, B_2,..., B_n. Notice that this change of Δ does not affect the location of the cubic curves such that the values of B_1, B_2,..., B_n remain intact. As a result of this procedure, we obtain the values B_i whose mean amplitude matches Condition 22 and yields the bridge amplitude A. Therefore, it remains to satisfy the phase balances (Eqs. 19 to 21) to identify the phases φ_i, i = 1,.., n, and ψ.

Comparing the phase balance conditions of Eqs. 19 and 21, we derive the following equations

$$\varphi_i + \bar{\varphi} = b_i, i = 1, \ldots, n \tag{23}$$

where $b_i = \arctan \lambda\frac{B_i^2 - a^2}{1-\omega_i^2} - \arctan\frac{2h}{\Omega^2 - 1}$ are known constants, given the fixed values of B_i and parameters λ, ω_i, h, and Ω. Because $\bar{\varphi} = \frac{1}{n}(\varphi_1 + \ldots + \varphi_n)$, finding φ_i, i = 1,..., n amounts to solving the system of n linear equations (Eq. 23). Therefore, the phases φ_i can be calculated even for a large crowd size n with only moderate effort. This will also allow us to calculate the mean phase $\bar{\varphi}$ and find the unknown bridge phase ψ via (Eq. 21)

$$\psi = \bar{\varphi} - \arctan\frac{2h}{1 - \Omega^2} \tag{24}$$

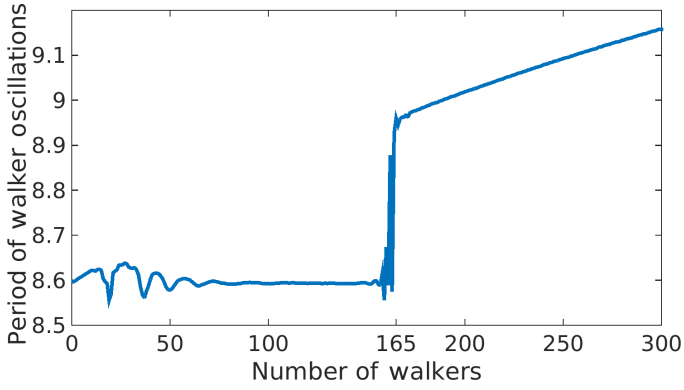

Fig. 6. Effect of bridge feedback on the period of walker oscillations. As the total mass of the pedestrian-bridge system increases with n, the period of phase-locked oscillations also increases.

The above procedure suggests a way of calculating the values of B_i, φ_i, A, and ψ and choosing the parameters of the pedestrian-bridge system (Eq. 5), which yield the phase-locked solutions $x_i(t)$ and $y(t)$ with frequency 1 and phases φ_i, which emerge when the crowd size reaches the critical value n_c. In this way, the distribution of $\omega_i = [\omega_-, \omega_+]$ translates into a distribution of phases φ_i that preserve the phase balances and the phase-locked solution with frequency equal to 1, similar to the identical pedestrian case. Although this procedure is direct, it gives implicit conditions for the existence and emergence of the phase-locked solutions and their dependence on the parameters of the pedestrian-bridge system. However, necessary conditions for the absence of the phase-locked solutions $x_i(t)$ and $y(t)$ can be given explicitly as follows.

Notice that the mean amplitude is $\bar{B} = \frac{1}{n}(B_1 + B_2 + \ldots + B_n)$ such that its square can be bounded by means of the Cauchy-Schwarz

inequality: $\bar{B}^2 = \frac{1}{n^2}(B_1 + B_2 + \ldots + B_n)^2 \le \frac{1}{n}(B_1^2 + B_2^2 + \ldots + B_n^2)$. Therefore, the balance equation (Eq. 20) can be turned into the inequality

$$A^2 \le \frac{(rn)^2}{\Delta}\left[\frac{1}{n}(B_1^2 + B_2^2 + \ldots + B_n^2)\right] = \frac{(rn)^2}{\Delta}\bar{B}^2 \qquad (25)$$

An elegant way to obtain the bounds that guarantee the absence of phase-locked solutions is to combine the amplitude balance equation (Eq. 18) and the inequality (Eq. 25)

$$\frac{(rn)^2}{\Delta}\left[\frac{1}{n}(B_1^2 + B_2^2 + \ldots + B_n^2)\right] \le B_i^2(\omega_i^2 - 1)^2 + \lambda(B_i^2 - a^2)^2 B_i^2 \qquad (26)$$

We use the lowest-frequency ω_- from the interval $\omega_i \in [\omega_-, \omega_+]$ and strengthen the inequality by replacing B_i^2 with the mean $\bar{B}^2$ on the RHS to obtain the lower bound curve for all B_i: $\frac{(rn)^2}{\Delta}\bar{B}^2 \le \bar{B}^2(\omega_-^2 - 1)^2 + \lambda(\bar{B}^2 - a^2)\bar{B}^2$. Consequently, we obtain the condition $\frac{(rn)^2}{\Delta} - (\omega_-^2 - 1)^2 \le \lambda(\bar{B}^2 - a^2)$. Notice that if the LHS of this inequality is less than 0, the inequality holds true for any amplitude $\bar{B}^2$. Therefore, we obtain the bound $\frac{(rn)^2}{\Delta} - (\omega_-^2 - 1)^2 < 0$, which is similar to that from the identical pedestrian case (Eq. 15) where the frequency ω is replaced with the lowest-frequency ω_-

$$\frac{mn^*}{mn^* + M} < |\omega_-^2 - 1|\sqrt{(\Omega^2 - 1)^2 + 4h^2} \qquad (27)$$

where n^* is the bound on the number of pedestrians below which the phase-locked solutions are absent and the wobbling of the bridge is practically 0 (cf. Fig. 7). Explicit in the parameters of the bridge, this condition can be used as a safety guideline for designing pedestrian bridges or limiting the maximum occupancy of an existing bridge. This also suggests that pedestrians with lower frequencies of their lateral gait are more prone to locking-in with the bridge motion.

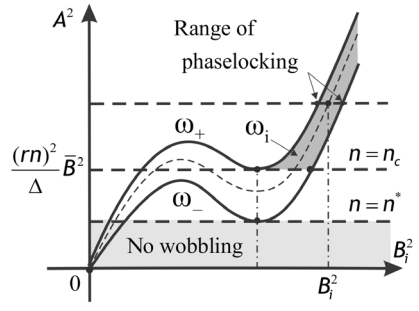

Fig. 7. Nonidentical oscillators with $\omega_i \in [\omega_-, \omega_+]$. Schematic diagram similar to the identical case of Fig. 2, where the cubic balance curve and inclined lines become a cubic strip and horizontal lines, respectively. The dark gray area denotes the range of phase locking, expressed through permissible amplitudes B_i and phases via Eqs. 22 and 23.

NONIDENTICAL INVERTED PENDULUM WALKERS

We return to the most realistic case of bioinspired inverted pendulum pedestrian-bridge model (Eqs. 1 to 3) with a 10% parameter mismatch (see Fig. 8). We randomly choose the parameters ω_i from the interval [0.6935, 0.7665], which is centered around $\omega = 0.73$ used in the above numerical simulations of the identical van der Pol–type pedestrian models (Eq. 5) (cf. Fig. 4). We choose other free individual pedestrian parameters as follows: $\lambda_i = \lambda = 2.8$, $p = 2$, and $a = 1$. This choice, together with the fixed parameters for the London Millennium Bridge (Figs. 4 and 8), gives the threshold value around $n_c = 160$. Therefore, we consistently obtain nearly the same threshold for both van der Pol–type and inverted pendulum models. It is worth noticing that numerical simulations of the inverted pendulum pedestrian-bridge model (Eqs. 1 to 3) with identical oscillators ($\omega_i = \omega = 0.73$) indicate the same threshold effect and nearly the same dependence of the bridge amplitude on the crowd size as in the nonidentical oscillator case of Fig. 8 (left) and therefore are not shown.

Figures 8 and 9 also indicate that well-developed phase locking is inevitably present when the number of pedestrians exceeds n_c; however, the abrupt initiation of bridge wobbling right at the edge of instability

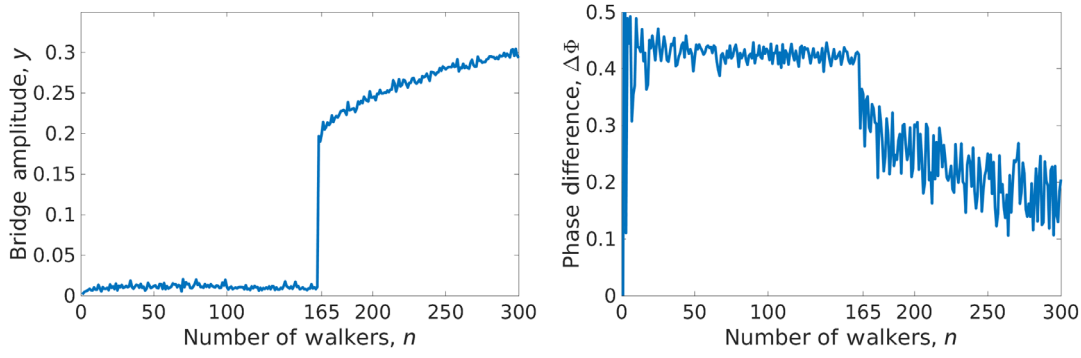

Fig. 8. Inverted pendulum model (Eqs. 1 to 3) of nonidentical pedestrians with randomly chosen parameters $\omega_i \in$ [0.6935, 0.7665] (10% mismatch). Diagrams similar to Fig. 4. The onset of bridge oscillations is accompanied by a drop in the average phase difference between the pedestrian's foot adjustment. The initial drop corresponding to the initiation of the bridge wobbling and partial phase locking is less significant, compared to the well-established phase locking at larger crowd sizes over 200 pedestrians. The individual pedestrian parameters are $\lambda = 2.8$, $p = 1$, and $a = 1$. Other parameters are as in Fig. 4. Models 1 to 3 with identical walkers produce similar curves with nearly the same critical crowd size; however, the phase difference drops to 0 (because complete phase locking is possible for identical oscillators).

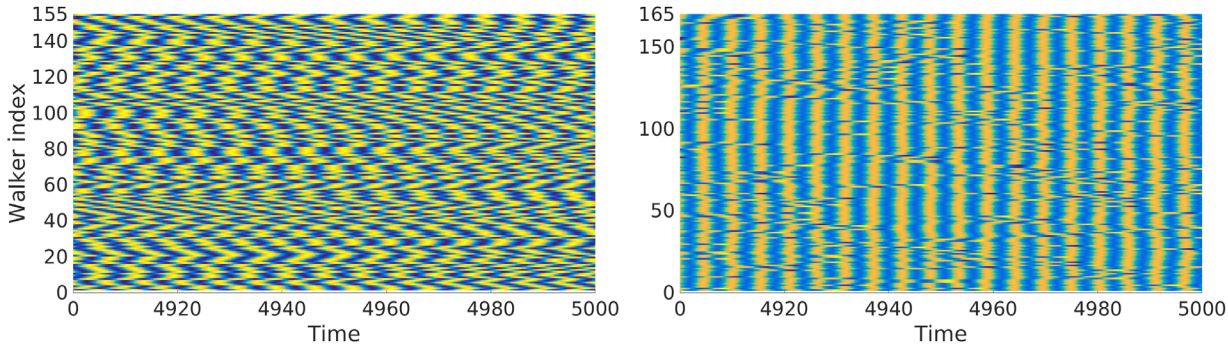

Fig. 9. Diagrams for the mismatched inverted pendulum pedestrian-bridge model (Eqs. 1 to 3), similar to Fig. 5. The full videos for both identical and mismatched inverted pendulum models are given in the Supplementary Materials.

around the critical number does not exactly coincide with total phase locking among the pedestrians and is accompanied by multiple phase slips and detuning. This suggests that pedestrian phase locking is crucial for a highly inertial system such as the London Millennium Bridge weighing over 113 tons to develop significant wobbling. However, its initiation mechanism at the edge of instability can be more complicated than simple phase locking. In particular, the balance control based on the lateral position of foot placement can initiate low-amplitude bridge wobbling before the onset of crowd synchrony at larger crowd sizes, as suggested by Macdonald (*46*).

CONCLUSION

The history of pedestrian and suspension bridges is full of dramatic events. The most recent examples are (i) the pedestrian-induced vibrations during the opening of the Solférino Bridge in Paris in 1999 (*28*) and the London Millennium Bridge in 2000 and (ii) the increased swaying of the Squibb Park Bridge in Brooklyn in 2014 (*34*) and the Volga Bridge (*56*) in the Russian city of Volgograd (formerly Stalingrad) (cost $396 million and 13 years to build), which experienced wind-induced resonance vibrations in 2011 soon after its opening and was shut down for expensive repairs. Parallels between wind and crowd loading of bridges have been widely discussed (*57*) because intensive research on the origin of resonant vibrations, caused by the pedestrian-bridge interaction and wind-induced oscillations, can have an enormous safety and economic impact.

Here, we have contributed toward understanding the dynamics of pedestrian locomotion and its interaction with the bridge structure. We have proposed two models where the individual pedestrian is represented by a biomechanically inspired inverted pendulum model (Eq. 3) and its simplified van der Pol–type analog. We have used the parameters close to those of the London Millennium Bridge to verify the popular explanation that the wobbling of London Millennium Bridge was initiated by phase synchronization of pedestrians falling into step with the bridge's oscillations. The analysis of both models has indicated the importance of the inclusion of foot force impacts for a more accurate prediction of the threshold effect. Surprisingly, the pedestrian-bridge system with a van der Pol–type oscillator as an individual pedestrian model allows for the rigorous analytical analysis of phase-locked solutions, although periodic solutions in the individual van der Pol–type oscillator cannot be found in closed form. Although we have used the van der Pol–type model of pedestrian gait to analytically elucidate the nontrivial relation between the pedestrians' and bridge dynamics, the numerical analysis of both the inverted pendulum and the van der Pol–type models reveals the same threshold effect for the sudden onset of bridge wobbling when the crowd size exceeds a critical value. This threshold effect is also present in the case of identical pedestrians such that a critical number of pedestrians are necessary for the bridge to abruptly develop significant wobbling. This is in contrast with the widespread view that identical pedestrians should always excite a bridge to wobble, with the amplitude of wobbling gradually increasing with the crowd size.

Our numerical study of the inverted pendulum pedestrian-bridge model confirms that crowd phase locking was necessary for the London Millennium Bridge to wobble significantly, especially at intermediate and large amplitudes. However, our simulations indicate that the initiation of wobbling is accompanied by tuning and detuning of pedestrian footstep such that a phase lock-in mechanism might not necessarily be the main cause of initial small-amplitude wobbling. A rigorous analysis of the inverted pendulum-bridge model to reveal secondary harmonics at which the wobbling can be initiated without total phase locking is a subject of future study.

The initiation of wobbling without crowd phase locking was previously observed during periods of instability of the Singapore Airport's Changi Mezzanine Bridge (*28*) and the Clifton Suspension Bridge (*32*). Both bridges experienced crowd-induced vibrations at a bridge frequency different from the averaged frequency of the pedestrians, while the pedestrians continued to walk without visible phase locking (*46*). Our recent results (*50*) on the ability of a single pedestrian to initiate bridge wobbling when switching from one gait to another may shed light on the initiation of small wobbling without crowd synchrony. More detailed models of pedestrian-bridge interaction that incorporate additional factors, such as, for example, an extra degree of freedom that accounts for the knee control in the individual pedestrian model and person-to-person visual communication and pace slowing in dense crowds, may also suggest an additional insight into the origin of this small-amplitude wobbling. From the dynamical systems perspective, this is an important piecewise smooth problem that requires careful mathematical study of the dynamics of nonsmooth oscillators (pedestrians), with the nonlinear coupling within the crowd and a bidirection interaction with a bridge structure.

Our theory and models should help engineers to better understand the dynamical impact of crowd collective behavior and guarantee the comfort level of pedestrians on a bridge. This requirement represents a major challenge because the natural frequency of an aesthetically pleasing lively bridge often falls into a critical frequency range of pedestrian

phase locking. These frequencies cannot be identified through the conventional linear calculations that might lead to faulty designs.

MATERIALS AND METHODS

Bounds for a limit cycle in the van der Pol–type walker model

In the absence of bridge movement ($\ddot{y} = 0$) in the pedestrian-bridge model (Eq. 5), the equation of motion for the ith pedestrian becomes

$$\ddot{x}_i + \lambda_i(\dot{x}_i^2 + x_i^2 - a^2)\dot{x}_i + \omega_i^2 x_i = 0 \qquad (28)$$

Applying the technique from Belykh *et al.* (*50*), we will prove the existence of a limit cycle in System 28 and give estimates on its frequency.

We introduce $V = \dot{x}^2 + \omega_i^2 x^2$ as a directing function for System 28. Its derivative along the trajectories of System 28 reads $\dot{V} = 2\dot{x}\ddot{x} + 2\omega_i^2 x\dot{x} = -2\lambda(\dot{x}_i^2 + x_i^2 - a^2)$. This derivative is 0 on the circle $C_1 : \{\dot{x}_i^2 + x_i^2 = a^2\}$ in the phase plane $(x_i, \dot{x}_i)$ of System 28 and is positive outside the circle C_1 and negative inside it. Without loss of generality, we assume that $\omega_i < 1$. We choose two levels of the directing function V: ellipses $V_1 = \dot{x}^2 + \omega_i^2 x^2 = a^2\omega_i^2$ and $V_2 = \dot{x}^2 + \omega_i^2 x^2 = a^2$, which inscribe and circumscribe the circle C_1, respectively. Therefore, the derivative $\dot{V}$ is positive (negative) on the level V_1 (V_2), except for the intersection points with the circle C_1 where $\dot{V} = 0$. As a result, the trajectories of System 28 enter the annulus $E = \{V_1 < V < V_2\}$, which contains a stable limit cycle. This claim also holds true for $\omega_i > 1$, with V_1 and V_2 interchanged.

Observe that $x = a \sin \omega_i t$ and $x = \frac{a}{\omega_i} \sin \omega_i t$ are solutions of the differential equations, governing V_1 and V_2, respectively. Hence, the frequency of rotation along the two curves is ω_i. Notice that the rotation along other level functions of V within E also has frequency ω_i. At the same time, the frequency of rotation along the circle C_1 equals 1, as $x = a \sin t$ is a solution of the differential equation $\dot{x}_i^2 + x_i^2 = a^2$, determining C_1. Although the limit cycle is bounded by the two level curves V_1 and V_2, it also intersects the circle C_1. Thus, its frequency lies within or near the interval $(\omega_i, 1)$. In the limiting case of $\omega_i \to 1$, the levels V_1 and V_2 and the circle C approach each other and merge; subsequently, the frequency of the limit cycle is 1. Notice that when the damping parameter λ is small, System 28 is nearly the harmonic oscillator, and therefore, the frequency of the limit cycle is close to ω_i. On the other hand, when λ is large and the van der Pol term becomes dominant, the frequency is close to 1.

Numerical simulations

All simulations were performed by integrating the systems of differential equations using an eighth-order Runge-Kutta method with a time step of 0.01. The number of equations for each simulation depends explicitly on the number of pedestrians on the bridge. To eliminate transient behaviors, numerical simulations were run for a final time on the order of 100 times the period of the bridge and pedestrian oscillations ($t_{\text{final}} = 5000$).

SUPPLEMENTARY MATERIALS

Supplementary material for this article is available at http://advances.sciencemag.org/cgi/content/full/3/11/e1701512/DC1

movie S1. Identical van der Pol.avi is related to Fig. 5.

movies S2 and S3. Inverted pendula identical.avi and inverted pendula 10% mismatch.avi are related to Fig. 9.

REFERENCES AND NOTES

1. C. Huygens, Letter to de Sluse, in *Oeuveres Complètes de Christian Huygens* (letters; no. 1333 of 24 February 1665, no. 1335 of 26 February 1665, no. 1345 of 6 March 1665) (Societe Hollandaise Des Sciences, Martinus Nijho, 1665).
2. M. Bennett, M. F. Schatz, H. Rockwood, K. Wiesenfeld, Huygens's clocks. *Proc. R. Soc. A Math. Phys. Eng. Sci.* **458**, 563–579 (2002).
3. A. Pikovsky, M. Rosenblum, J. Kurths, *Synchronization: A Universal Concept in Nonlinear Sciences* (Cambridge Univ. Press, 2003), vol. 12.
4. J. Peña Ramirez, L. A. Olvera, H. Nijmeijer, J. Alvarez, The sympathy of two pendulum clocks: Beyond Huygens' observations. *Sci. Rep.* **6**, 23580 (2016).
5. E. V. Pankratova, V. N. Belykh, Consequential noise-induced synchronization of indirectly coupled self-sustained oscillators. *Eur. Phys. J. Spec. Top.* **222**, 2509–2515 (2013).
6. V. N. Belykh, E. V. Pankratova, A. Y. Pogromsky, H. Nijmeijer, Two Van der Pol-Duffing oscillators with Huygens coupling, in *Dynamics and Control of Hybrid Mechanical Systems*, G. A. Leonov, H. Nijmeijer, A. Y. Pogromsky, A. L. Fradkov, Eds. (World Scientific Publishing Co. Pte. Ltd., 2010), pp. 181–194.
7. L. M. Pecora, T. L. Carroll, Master stability functions for synchronized coupled systems. *Phys. Rev. Lett.* **80**, 2109 (1998).
8. S. H. Strogatz, Exploring complex networks. *Nature* **410**, 268–276 (2001).
9. S. Boccaletti, J. Kurths, G. Osipov, D. L. Valladares, C. S. Zhou, The synchronization of chaotic systems. *Phys. Rep.* **366**, 1–101 (2002).
10. V. N. Belykh, I. V. Belykh, M. Hasler, Connection graph stability method for synchronized coupled chaotic systems. *Physica D* **195**, 159–187 (2004).
11. T. Nishikawa, A. E. Motter, Network synchronization landscape reveals compensatory structures, quantization, and the positive effect of negative interactions. *Proc. Natl. Acad. Sci. U.S.A.* **107**, 10342–10347 (2010).
12. A. J. Whalen, S. N. Brennan, T. D. Sauer, S. J. Schiff, Observability and controllability of nonlinear networks: The role of symmetry. *Phys. Rev. X* **5**, 011005 (2015).
13. J. J. Collins, I. N. Stewart, Coupled nonlinear oscillators and the symmetries of animal gaits. *J. Nonlinear Sci.* **3**, 349–392 (1993).
14. L. Glass, M. C. Mackey, *From Clocks to Chaos: The Rhythms of Life* (Princeton Univ. Press, 1988).
15. M. E. J. Newman, The structure and function of complex networks. *SIAM Rev.* **45**, 167–256 (2003).
16. A. E. Motter, S. A. Myers, M. Anghel, T. Nishikawa, Spontaneous synchrony in power-grid networks. *Nat. Phys.* **9**, 191–197 (2013).
17. I. V. Belykh, M. Porfiri, Introduction: Collective dynamics of mechanical oscillators and beyond. *Chaos* **26**, 116101 (2016).
18. Wikipedia, List of bridge failures, https://en.wikipedia.org/wiki/List_of_bridge_failures.
19. S. Živanović, A. Pavic, P. Reynolds, Vibration serviceability of footbridges under human-induced excitation: A literature review. *J. Sound Vib.* **279**, 1–74 (2005).
20. V. Racic, A. Pavic, J. M. W. Brownjohn, Experimental identification and analytical modelling of human walking forces: Literature review. *J. Sound Vib.* **326**, 1–49 (2009).
21. F. Venuti, L. Bruno, Crowd-structure interaction in lively footbridges under synchronous lateral excitation: A literature review. *Phys. Life Rev.* **6**, 176–206 (2009).
22. F. B. Farquharson, F. C. Smith, G. S. Vincent, Eds., *Aerodynamic Stability of Suspension Bridges with Special Reference to the Tacoma Narrows Bridge* (Bulletin 116, University of Washington Engineering Experiment Station, 1950).
23. K. Y. Billah, R. H. Scanlan, Resonance, Tacoma Narrows bridge failure, and undergraduate physics textbooks. *Am. J. Phys.* **59**, 118–124 (1991).
24. D. Green, W. G. Unruh, The failure of the Tacoma Bridge: A physical model. *Am. J. Phys.* **74**, 706–716 (2006).
25. E. H. Dowell, R. Clark, *A Modern Course in Aeroelasticity: Solid Mechanics and Its Applications* (Springer Science and Business Media, 2004).
26. G. Arioli, F. Gazzola, A new mathematical explanation of what triggered the catastrophic torsional mode of the Tacoma Narrows Bridge. *Appl. Math. Model.* **39**, 901–912 (2015).
27. Y. Fujino, B. M. Pacheco, S.-I. Nakamura, P. Warnitchai, Synchronization of human walking observed during lateral vibration of a congested pedestrian bridge. *Earthq. Eng. Struct. Dyn.* **22**, 741–758 (1993).
28. F. Danbon, G. Grillaud, Dynamic behaviour of a steel footbridge. Characterization and modelling of the dynamic loading induced by a moving crowd on the Solferino Footbridge in Paris, in *Proceedings of Footbridge 2005*, 6 to 8 December 2005 (Second International Congress, 2005).
29. P. Dallard, A. Fitzpatrick, A. Flint, S. Le Bourva, A. Low, R. Ridsdill Smith, M. Willford, The London millennium footbridge. *Struct. Eng.* **79**, 17–21 (2001).
30. S.-I. Nakamura, Field measurements of lateral vibration on a pedestrian suspension bridge. *Struct. Eng.* **81**, 22–26 (2003).
31. J. M. W. Brownjohn, P. Fok, M. Roche, P. Omenzetter, Long span steel pedestrian bridge at Singapore Changi Airport. Part 2: Crowd loading tests and vibration mitigation measures. *Struct. Eng.* **82**, 21–27 (2004).
32. J. H. G. Macdonald, Pedestrian-induced vibrations of the Clifton Suspension Bridge, UK, in *Proceedings of the Institution of Civil Engineers-Bridge Engineering* (Thomas Telford Ltd., 2008), vol. 161, pp. 69–77.

33. E. Caetano, Á. Cunha, F. Magalhães, C. Moutinho, Studies for controlling human-induced vibration of the Pedro e Inês footbridge, Portugal. Part 1: Assessment of dynamic behaviour. *Eng. Struct.* **32**, 1069–1081 (2010).
34. R. Woodward, T. Zoli, Two bridges built using black locust wood, in *Proceedings of the International Conference on Timber Bridges*, 30 September to 2 October (2013).
35. L. W. Foderaro, "A new bridge bounces too far and is closed until the spring," *New York Times*, 3 October 2014.
36. L. W. Foderaro, "Brooklyn walkway to reopen, with less bounce in your steps," *New York Times*, 17 April 2017.
37. A. Plitt, "Brooklyn bridge park's squibb park bridge reopens with slightly less bounce," *Curbed New York*, 19 April 2017.
38. S.-i. Nakamura, Model for lateral excitation of footbridges by synchronous walking. *J. Struct. Eng.* **130**, 32–37 (2004).
39. G. Piccardo, F. Tubino, Parametric resonance of flexible footbridges under crowd-induced lateral excitation. *J. Sound Vib.* **311**, 353–371 (2008).
40. S. H. Strogatz, D. M. Abrams, A. McRobie, B. Eckhardt, E. Ott, Theoretical mechanics: Crowd synchrony on the Millennium Bridge. *Nature* **438**, 43–44 (2005).
41. B. Eckhardt, E. Ott, S. H. Strogatz, D. M. Abrams, A. McRobie, Modeling walker synchronization on the Millennium Bridge. *Phys. Rev. E* **75**, 021110 (2007).
42. M. M. Abdulrehem, E. Ott, Low dimensional description of pedestrian-induced oscillation of the Millennium Bridge. *Chaos* **19**, 013129 (2009).
43. M. Bocian, J. H. G. Macdonald, J. F. Burn, Biomechanically inspired modelling of pedestrian-induced forces on laterally oscillating structures. *J. Sound Vib.* **331**, 3914–3929 (2012).
44. LRFD, *Guide Specifications for the Design of Pedestrian Bridges* (American Association of State Highway and Transportation Officials, 2009).
45. C. Barker, Some observations on the nature of the mechanism that drives the self-excited lateral response of footbridges, in *Proceedings of the International Conference on the Design and Dynamic Behaviour of Footbridges*, 20 to 22 November (2002).
46. J. H. G. Macdonald, Lateral excitation of bridges by balancing pedestrians. *Proc. R. Soc. London Ser. A* **465**, 1055–1073 (2008).
47. A. Hof, R. M. van Bockel, T. Schoppen, K. Postema, Control of lateral balance in walking: Experimental findings in normal subjects and above-knee amputees. *Gait Posture* **25**, 250–258 (2007).
48. A. L. Hof, S. M. Vermerris, W. Gjaltema, Balance responses to lateral perturbations in human treadmill walking. *J. Exp. Biol.* **213**, 2655–2664 (2010).
49. C. D. MacKinnon, D. A. Winter, Control of whole body balance in the frontal plane during human walking. *J. Biomech.* **26**, 633–644 (1993).
50. I. V. Belykh, R. Jeter, V. N. Belykh, Bistable gaits and wobbling induced by pedestrian-bridge interactions. *Chaos* **26**, 116314 (2016).
51. T. Heath, K. Wiesenfeld, Synchronization transitions in Josephson arrays: A puzzle and its resolution. *Ann. Phys.* **9**, 689–696 (2000).
52. J. A. Acebrón, L. L. Bonilla, C. J. P. Vicente, F. Ritort, R. Spigler, The Kuramoto model: A simple paradigm for synchronization phenomena. *Rev. Mod. Phys.* **77**, 137 (2005).
53. D. M. Abrams, S. H. Strogatz, Chimera states for coupled oscillators. *Phys. Rev. Lett.* **93**, 174102 (2004).
54. E. A. Martens, S. Thutupalli, A. Fourrière, O. Hallatschek, Chimera states in mechanical oscillator networks. *Proc. Natl. Acad. Sci. U.S.A.* **110**, 10563–10567 (2013).
55. K. Blaha, R. J. Burrus, J. L. Orozco-Mora, E. Ruiz-Beltrán, A. B. Siddique, V. D. Hatamipour, F. Sorrentino, Symmetry effects on naturally arising chimera states in mechanical oscillator networks. *Chaos* **26**, 116307 (2016).
56. M. Brun, A. Movchan, I. Jones, R. McPhedran, Bypassing shake, rattle and roll. *Phys. World* **26**, 32 (2013).
57. A. McRobie, G. Morgenthal, D. Abrams, J. Prendergast, Parallels between wind and crowd loading of bridges. *Philos. Trans. A Math. Phys. Eng. Sci.* **371**, 20120430 (2013).

Acknowledgments: We acknowledge guidance with existing bioinspired inverted pendulum models of pedestrian gait and the role of balance control from A. Champneys and J. Macdonald, both from the University of Bristol, U.K. We thank D. Feliciangeli, a bridge engineer with Mott Macdonald Group, for pointing us to the U.S. Guide Specifications for the design of pedestrian bridges and useful discussions. **Funding:** This work was supported by the U.S. National Science Foundation under grant no. DMS-1616345 (to I.B. and R.J.), the Russian Science Foundation under grant no. 14-12-00811, and the Russian Foundation for Fundamental Research under grant no. 15-01-08776 (to V.B.). **Author contributions:** I.B. conceived the project and drafted the manuscript. I.B. and V.B. developed the models and contributed to their theoretical analysis. R.J. performed simulations. All authors contributed to the editing of the manuscript. **Competing interests:** The authors declare that they have no competing interests. **Data and materials availability:** All data needed to evaluate the conclusions in the paper are present in the paper and/or the Supplementary Materials. Additional data related to this paper may be requested from the authors.

Submitted 9 May 2017
Accepted 18 October 2017
Published 10 November 2017
10.1126/sciadv.1701512

Citation: I. Belykh, R. Jeter, V. Belykh, Foot force models of crowd dynamics on a wobbly bridge. *Sci. Adv.* **3**, e1701512 (2017).